

## Supporting Information

### Dual Carbon-Modified Nickel Sulfide Composites Toward High-Performance Electrodes for Supercapacitors

Jiapeng He<sup>a</sup>, Can Guo<sup>a</sup>, Shaowen Zhou<sup>a</sup>, Yinlong Zhao<sup>a</sup>, Qingpeng Wang<sup>c</sup>, Shun Yang<sup>a,\*</sup>, Jiaqin Yang<sup>b,\*</sup>, Qinghong Wang<sup>a,\*</sup>

<sup>a</sup> School of Chemistry and Materials Science, Jiangsu Normal University, Xuzhou 221116, China.

<sup>b</sup> School of Chemistry and Chemical Engineering, Qufu Normal University, Qufu 273165, China.

<sup>c</sup> Institute of Biopharmaceutical Research, Liaocheng University, Liaocheng 252059, China.

E-mail: [yangshun@jsnu.edu.cn](mailto:yangshun@jsnu.edu.cn) (S. Yang), [yjq8681@163.com](mailto:yjq8681@163.com) (J. Q. Yang),

[wangqh@jsnu.edu.cn](mailto:wangqh@jsnu.edu.cn) (Q. H. Wang)

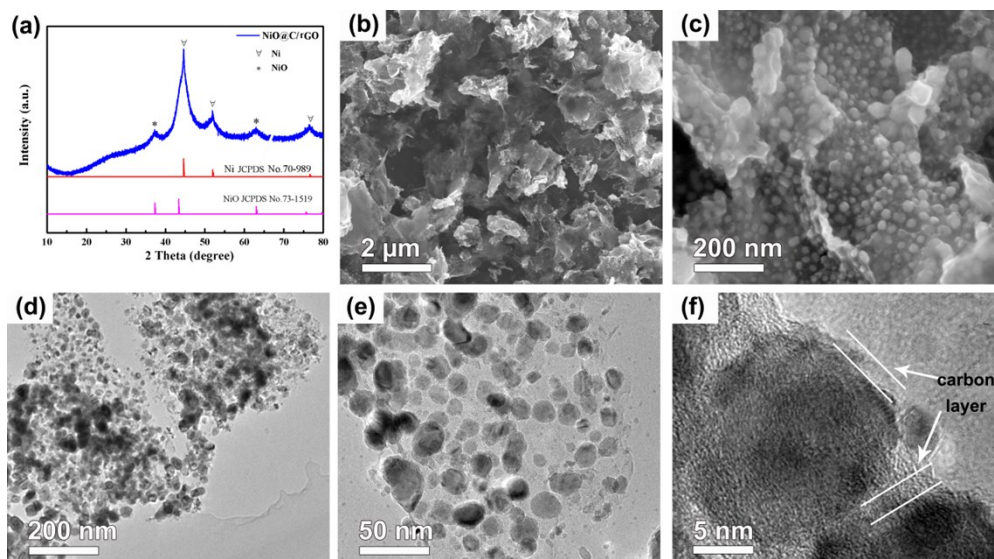


**Figure S1.** (a) XRD pattern, (b, c) SEM images and (d-f) TEM images of NiO@C/rGO precursor.

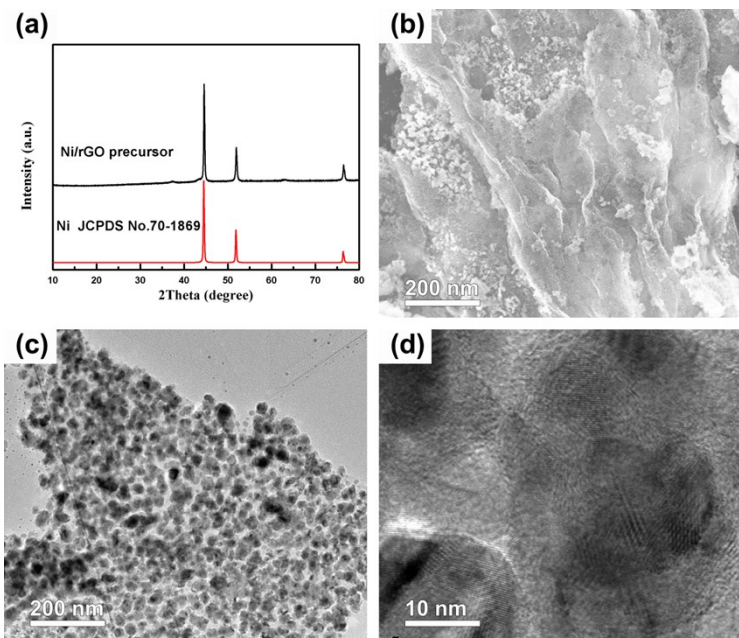


**Figure S2.** (a) XRD pattern, (b) SEM image and (c, d) TEM images of Ni/rGO precursor.

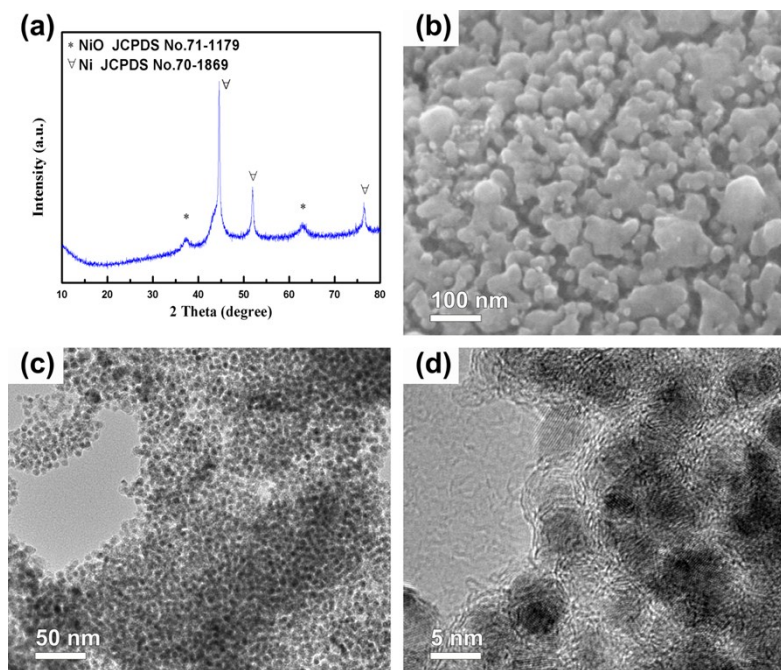


**Figure S3.** (a) XRD pattern, (b) SEM image and (c, d) TEM images of NiO@C precursor.

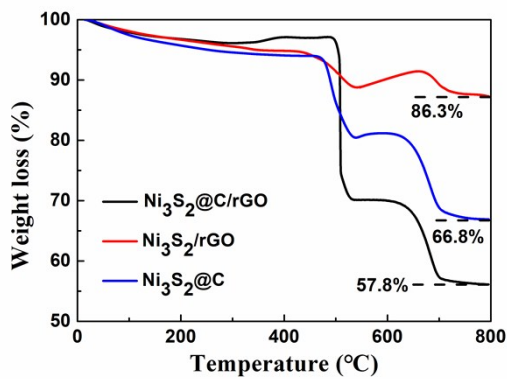


**Figure S4.** TGA curves of the as-prepared  $\text{Ni}_3\text{S}_2@\text{C}/\text{rGO}$ ,  $\text{Ni}_3\text{S}_2/\text{rGO}$  and  $\text{Ni}_3\text{S}_2@\text{C}$  composites.

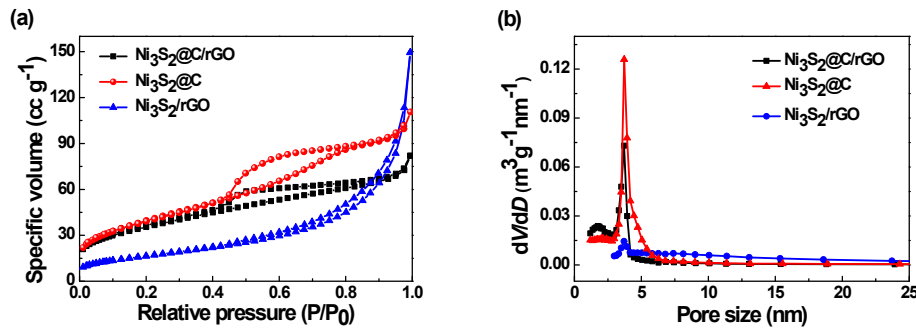


**Figure S5.** (a) N<sub>2</sub> adsorption-desorption isotherms and (b) pore size distributions of the as-prepared  $\text{Ni}_3\text{S}_2@\text{C}/\text{rGO}$ ,  $\text{Ni}_3\text{S}_2/\text{rGO}$  and  $\text{Ni}_3\text{S}_2@\text{C}$  composites.

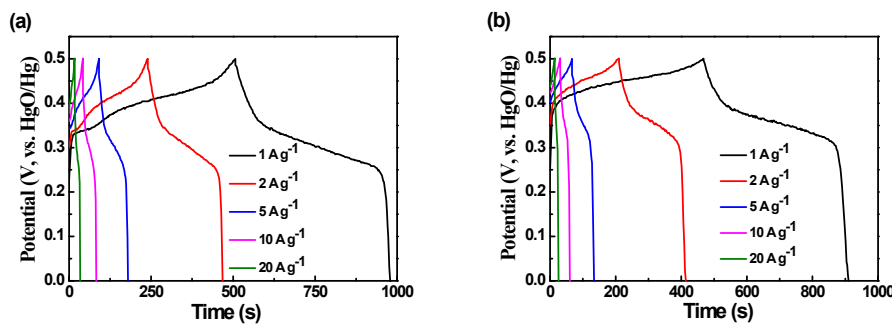


**Figure S6.** Charge-discharge curves of (a)  $\text{Ni}_3\text{S}_2/\text{rGO}$  and (b)  $\text{Ni}_3\text{S}_2@\text{C}$  electrodes at different current densities.

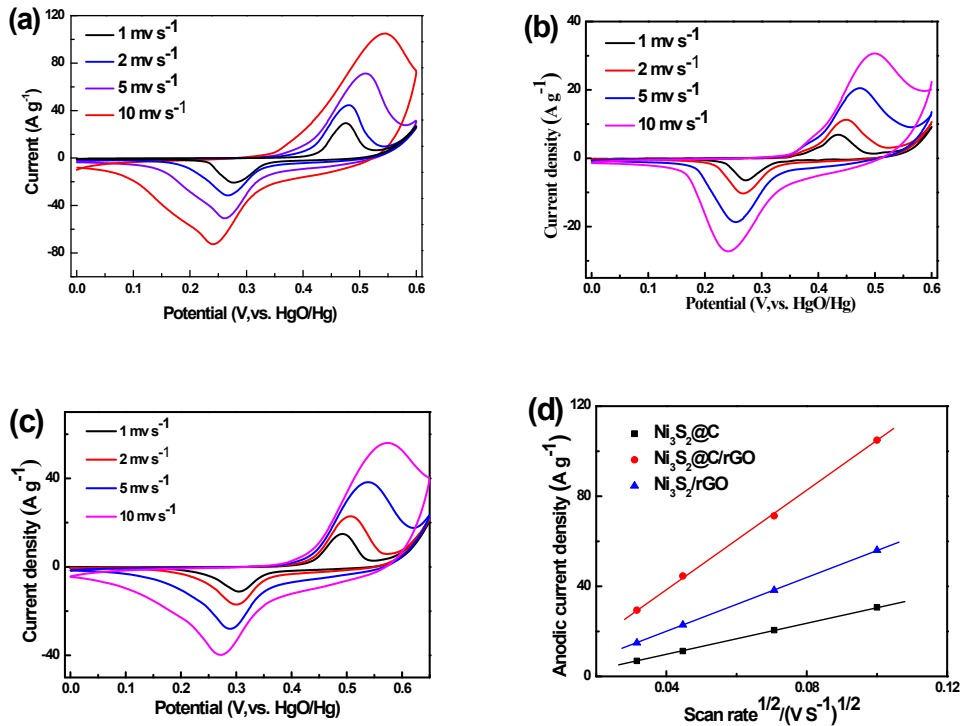


**Figure S7.** CV curves of the (a)  $\text{Ni}_3\text{S}_2@\text{C}/\text{rGO}$ , (b)  $\text{Ni}_3\text{S}_2@\text{C}$  and (c)  $\text{Ni}_3\text{S}_2/\text{rGO}$  electrode at different scan rates. (d) Dependence of the peak current density on square root of sweep rate for the as-prepared  $\text{Ni}_3\text{S}_2$  electrodes (cathodic peaks).

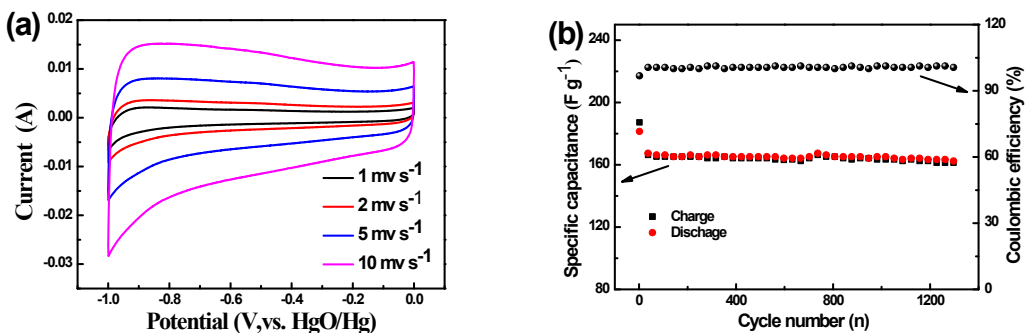


**Figure S8.** (a) CV curves of the AC electrode at different scan rates. (b) Cycle performance of AC electrode at 5  $\text{A g}^{-1}$ .

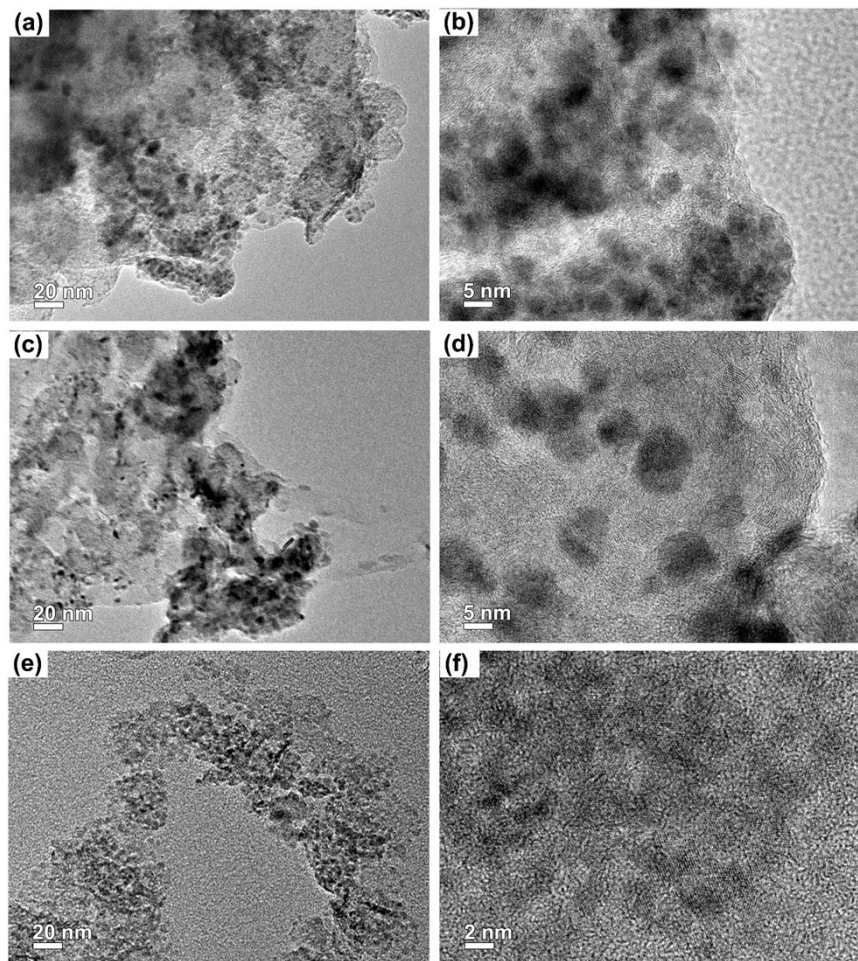


**Figure S9.** TEM images of (a, b)  $\text{Ni}_3\text{S}_2@\text{C}/\text{rGO}$ , (c, d)  $\text{Ni}_3\text{S}_2@\text{C}$  and (e, f)  $\text{Ni}_3\text{S}_2/\text{rGO}$  electrodes after 1000 cycles at  $5 \text{ A g}^{-1}$ .

**Table S1** Rate performance of Ni<sub>3</sub>S<sub>2</sub>@C/rGO, Ni<sub>3</sub>S<sub>2</sub>@C and Ni<sub>3</sub>S<sub>2</sub>/rGO electrodes at different current densities

Current density (A g <sup>-1</sup> )	Ni <sub>3</sub> S <sub>2</sub> @C/rGO (F g <sup>-1</sup> )	Ni <sub>3</sub> S <sub>2</sub> /rGO (F g <sup>-1</sup> )	Ni <sub>3</sub> S <sub>2</sub> @C (F g <sup>-1</sup> )
1	1171	980	910
2	1107	936	830
5	1023	900	670
10	936	830	620
20	848	680	510